SCIENTIFIC REPORTS

OPEN

SUBJECT AREAS:
THERMOELECTRICS
APPLIED PHYSICS
MATERIALS FOR DEVICES
ELECTRONICS, PHOTONICS AND DEVICE PHYSICS

Received
8 January 2013

Accepted
1 March 2013

Published
20 March 2013

Correspondence and requests for materials should be addressed to K.T. (kohei.takahashi@jp.panasonic.com)

Bifunctional thermoelectric tube made of tilted multilayer material as an alternative to standard heat exchangers

Kouhei Takahashi, Tsutomu Kanno, Akihiro Sakai, Hiromasa Tamaki, Hideo Kusada & Yuka Yamada

Advanced Technology Research Laboratories, Panasonic Corporation, 3-4 Hikaridai, Seika-cho, Soraku-gun, Kyoto 619-0237, Japan.

Enormously large amount of heat produced by human activities is now mostly wasted into the environment without use. To realize a sustainable society, it is important to develop practical solutions for waste heat recovery. Here, we demonstrate that a tubular thermoelectric device made of tilted multilayer of $Bi_{0.5}Sb_{1.5}Te_3$/Ni provides a promising solution. The $Bi_{0.5}Sb_{1.5}Te_3$/Ni tube allows tightly sealed fluid flow inside itself, and operates in analogy with the standard shell and tube heat exchanger. We show that it achieves perfect balance between efficient heat exchange and high-power generation with a heat transfer coefficient of 4.0 kW/m^{2}K and a volume power density of 10 kW/m^3 using low-grade heat sources below 100°C. The $Bi_{0.5}Sb_{1.5}Te_3$/Ni tube thus serves as a power generator and a heat exchanger within a single unit, which is advantageous for developing new cogeneration systems in factories, vessels, and automobiles where cooling of excess heat is routinely carried out.

Growing energy consumption and the associated environmental damage have made our focuses on renewable energy resources. Among them, efficient usage of exhaust heat is demanded in various scenes, for example, in factories, waste incineration plants, data centers, and even in hot springs. In many of these facilities, excess heat is forced to cool down to adequate temperatures with the help of devices called "heat exchangers." The thermal energy consumed in this cooling process is enormous, and unfortunately, mostly wasted, but the process itself is highly essential for many reasons such as safety, environmental conservation, and performance retention of various apparatus including engines and turbines. One of the potential solutions for waste heat recovery in these systems is the use of Seebeck effect in thermoelectric (TE) materials[1–5]. In TE materials, Seebeck effect generates a voltage signal between two arbitrary points by introducing a temperature difference ΔT. Thus, attaching one side of the TE device to the exhaust heat and the other side to a coolant enables electric power generation with an output proportional to ΔT^2. However, it should be noticed that the conventional TE devices are normally designed with high thermal resistances to sustain large-ΔT. This means that cooling of exhaust heat, which has higher priority than additional power generation in the abovementioned facilities, will be inhibited by the introduction of TE devices. Innovation in material/device performance is thus necessary for application of TE conversion in waste heat recovery systems.

Lately, unconventional approaches have been applied in the field of thermoelectrics to improve their performances. Nanotechnology is a major example[3–8]. Another example is the transverse TE effect, or the off-diagonal TE effect, which essentially develops in tilted layered materials[9–18]. The previous studies have revealed various unusual phenomena arising from this effect including the gigantic voltage generation in incline-oriented nanometer-scale thin films[9–11], and enhanced power factors in artificial tilted multilayer materials[17]. Transverse TE devices exhibit distinct functions as compared to the ordinary TE devices as follows; (i) the voltage signal develops perpendicular to the applied ΔT (see the schematic in Fig. 1a)[9–18], (ii) compatibility between n-type and p-type TE material[19] is not necessary since either of them is sufficient to construct the device (the polarity of the TE voltage can be reversed by reversing the tilt-direction of the layers), and (iii) the macroscopic physical properties of the multilayer material can be tuned widely by changing the combination and the periodicity of the constituents[12–18]. These features provide us new degree of freedom in designing alternative TE devices. In fact, we have recently fabricated a multilayer of $Bi_{0.5}Sb_{1.5}Te_3$ (BST) and Ni in a tubular device structure by alternately solder-pasting casted rings of BST and Ni[20]. The cross-section of the BST/Ni tube demonstrated that a tilted multilayer of BST and Ni was indeed realized in this structure. Reflecting the tilted layered structure, we found that a voltage signal uniquely develops in the tube-axial direction by introducing ΔT between the inner side and the outer side of the

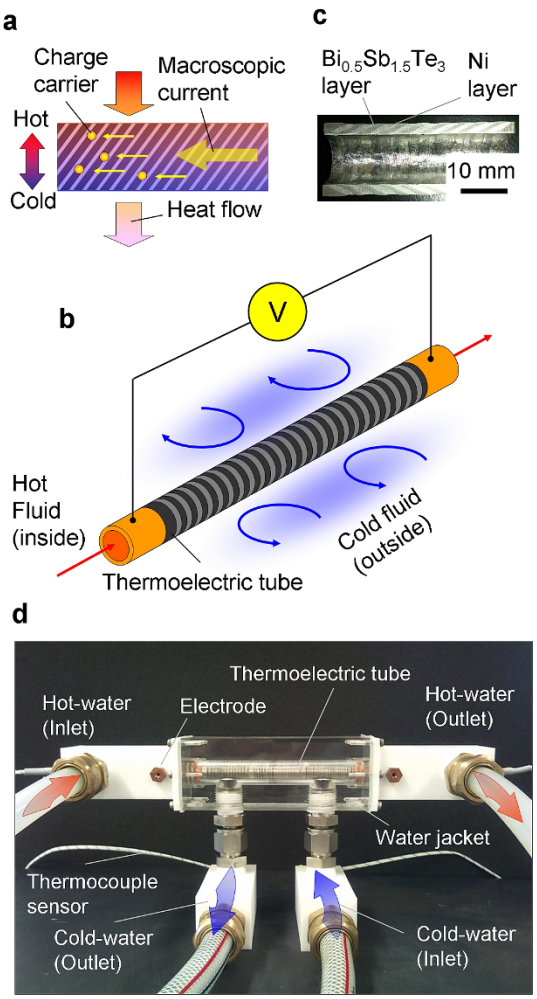

Figure 1 | Operation environment of the tubular TE device made of tilted layered material. (a) Schematic of the transverse TE (off-diagonal TE) effect in a tilted layered material. The voltage develops perpendicular to the applied temperature gradient. (b) Schematic of the operation of the TE tube. Temperature difference along the tube radial direction generates an electric signal along the tube axial direction. (c) Cross-sectional picture of the BST/Ni tube. The tilted stripes at the top and the bottom represent the tilted layered structure of BST and Ni. (d) Picture of the experimental setup to evaluate the heat exchange properties and the power generation properties of the TE tube.

tube. Namely, the BST/Ni tube can generate electricity by running hot fluid inside the tube and immersing itself inside cold fluid as shown in Fig. 1b. The peculiar tubular shape is practical, which allows the BST/Ni tube to serve as one of the plumbing components in water supply lines in various facilities.

Here, we report progressive results on the heat exchange properties and the power generation properties of a BST/Ni TE tube, which was newly fabricated by an advanced spark plasma sintering (SPS) technique. The BST/Ni tube examined here exhibited dense and firm structure with well-ordered joints of BST and Ni, enabling tightly sealed fluid flow inside itself. Measurements at various water flow conditions manifested efficient heat exchange and simultaneous high electric power generation from the BST/Ni tube. The bifunctional BST/Ni tube shall provide practical waste heat recovery solution as an alternative to the existing heat exchangers.

Results

11 cm-long BST/Ni multilayer tube with an outer diameter and an inner diameter of 14 mm and 10 mm, respectively, was fabricated by SPS technique using powders of BST and Ni as starting materials. The tilt angle and the thickness of each BST/Ni layers were ~35° and ~1.3 mm, respectively (see the cross-sectional picture in Fig. 1c). The electrical resistance R_e of the BST/Ni tube was ~4.5 mΩ. Figure 1d shows the picture of the experimental equipment to measure the heat exchange properties and the electric power generation properties of the BST/Ni tube. The BST/Ni tube was placed inside an acrylic water jacket with a ϕ18 mm-flow channel. Hot-water was introduced inside the BST/Ni tube, while the outer side was cooled by introducing cold-water inside the acrylic water jacket. The operation environment of the BST/Ni tube explained here is similar to that of the standard shell and tube heat exchangers. We confirmed that the BST/Ni tube was sealed tightly and that there was no direct intermixing between the hot-water and the cold-water.

Figure 2a shows typical example of the electric power generation characteristics of the BST/Ni tube measured by introducing hot-water of 95°C and cold-water of 10°C, both at a flow rate of 20 L/min. The closed squares and the closed circles represent the current-voltage plot and the power-voltage plot, respectively. The linear fit and the quadratic fit to each curve are also shown by the solid lines. One can see that the open circuit voltage V_{op} is 0.24 V and the maximum electric power P_e generated at a load matching condition is 2.7 W, which corresponds to a power density of 870 W/m^2 of heat transfer area. V_{op} is rather low, but the low-R_e of the tube enables generation of high-P_e from the low-grade heat sources at temperatures below 100°C. Figure 2b shows V_{op} measured as a function of hot-water temperature T_{hw} at fixed cold-water temperature T_{cw} of 10°C. The closed squares are the data and the solid line is a linear fit to the data. We see that V_{op} decreases linearly with decreasing T_{hw}, and approaches to zero when T_{hw} approaches to 10°C. This clearly

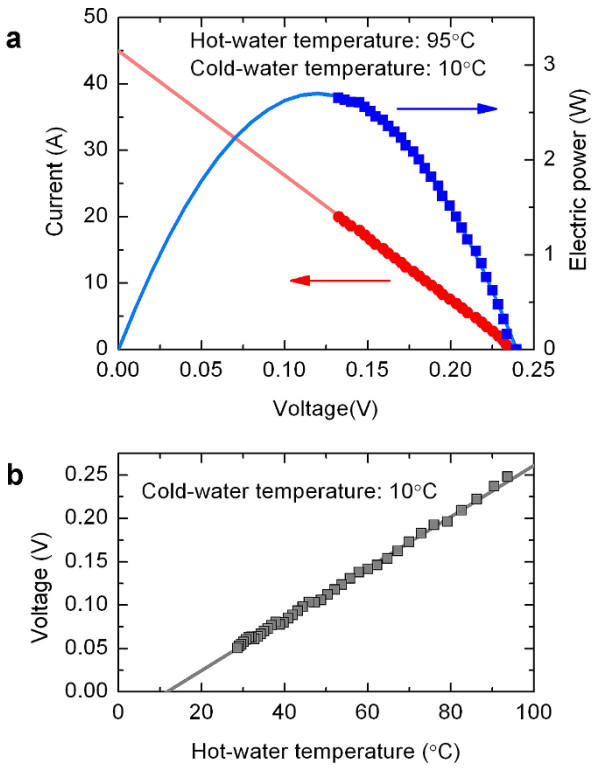

Figure 2 | TE generation property of the BST/Ni multilayer tube. (a) Current-voltage plot (closed squares) and power-voltage plot (closed circles) of the BST/Ni tube measured by introducing hot-water of 95°C and cold-water of 10°C at F_{cw} and F_{hw} of 20 L/min. The linear fit and the quadratic fit to each data are also shown by the solid lines. (b) V_{op} of the BST/Ni tube measured as a function of T_{hw}. Note that T_{cw} is fixed at 10°C and F_{cw} and F_{hw} is both fixed at 20 L/min.

shows that the voltage signal is in direct relation with ΔT established between the inner side and the outer side of the tube.

The heat exchange properties and the electric power generation properties of the BST/Ni tube measured at various hot-water flow rate F_{hw} and cold-water flow rate F_{cw} are summarized in Figs. 3a–3e. Note that T_{hw} and T_{cw} is fixed at 95°C and 10°C, respectively. Figure 3a shows contour map of V_{op} measured as a function of F_{hw} and F_{cw}. Although T_{hw} and T_{cw} are fixed, we see that V_{op} varies significantly from 0.15 to 0.24 V with increasing F_{hw} and F_{cw} from 4 to 20 L/min. Accordingly, P_e at load matching condition also increases from 1.0 to 2.7 W as depicted in Fig. 3b. The temperature difference T_{diff} between the inlet and the outlet T_{cw} (i.e., the temperature rise of the cold-water after passing the BST/Ni tube) is also plotted as a function of F_{hw} and F_{cw} in Fig. 3c. Note that T_{diff} of the hot-water (not shown) was several percent larger than that of the cold-water presumably due to additional heat exchange between the hot-water and the environment. As seen in Fig. 3c, T_{diff} changes from 0.7 to 3.5°C with varying F_{cw} and F_{hw}. The relatively large T_{diff} of 3.5°C achieved here from the short 11 cm tube demonstrates the excellent heat exchange property of the BST/Ni tube. Using the measured T_{diff} values, we have calculated the thermal power Q exchanged by the 11 cm tube at each water flow conditions. Defining C_w and ρ_w as the heat capacity and density of water, Q can be expressed as,

$$Q = C_w \rho_w F_{cw} T_{diff}. \quad (1)$$

The F_{hw} and F_{cw} dependence of Q is shown by a contour map in Fig. 3d. Similar to the other parameters, Q changes significantly with varying F_{hw} and F_{cw}. Most notable is the large magnitude of Q, which exceeds 1 kW at F_{hw} and F_{cw} above 10 L/min. This corresponds to heat flux of more than 230 kW/m^2. The heat transfer coefficient α of the BST/Ni tube can be calculated as,

$$\alpha = \frac{Q}{A(T_{hw} - T_{cw})}, \quad (2)$$

where A is the heat transfer area. Based on the measured Q values, α is calculated to be as large as 4.0 kW/m^{2}K. This is only about half the value (or the same) when a pure Cu tube (or a stainless-steel tube) is substituted into this system, but more than 5 times larger than that achieved by the conventional "π-shaped" TE devices, which represents that effective heat exchange can indeed be realized by the BST/Ni tube. The conversion efficiency η of the BST/Ni tube was also estimated by using the measured quantities as, $\eta = P_e/Q$. The contour map of η plotted as a function of F_{hw} and F_{cw} is depicted in Fig. 3e. The present measurement show that η of the BST/Ni tube is relatively low ranging from 0.12–0.19% depending on the water flow rate.

The F_{hw} and F_{cw} dependences in Figs. 3a–3e demonstrate that the BST/Ni tube exhibits higher performances at larger water flow rates. This tendency can be understood well by considering the change in thermal resistance R_t. In the present setup, R_t between hot-water and cold-water can be divided into three components, i.e., (i) the interface-R_t between the cold-water and the outer side of the tube, (ii) bulk-R_t of the tube, and (iii) interface-R_t between the inner side of the tube and the hot-water. The increase in F_{hw} and F_{cw} essentially reduces the interface-R_t at each side, which makes the bulk-R_t of the tube more dominant among the overall-R_t. As a result, heat exchange is promoted at larger F_{hw} and F_{cw}, which increases Q introduced into the BST/Ni tube. This eventually increases ΔT between the inner side and the outer side of the BST/Ni tube, and hence, generates larger V_{op} and P_e at larger water flow rates. The present result provides a primary guideline for designing large-scale TE generation unit from the given supply rate of the heat source, for example, on the optimal numbers and length of the BST/Ni tube that achieves highest P_e.

For further demonstration, we have fabricated a compact prototypical TE generation unit made of four BST/Ni tubes. Figure 4a shows the picture of the TE generation unit. Four numbers of 11 cm-long BST/Ni tubes are built-in the TE generation unit. The BST/Ni

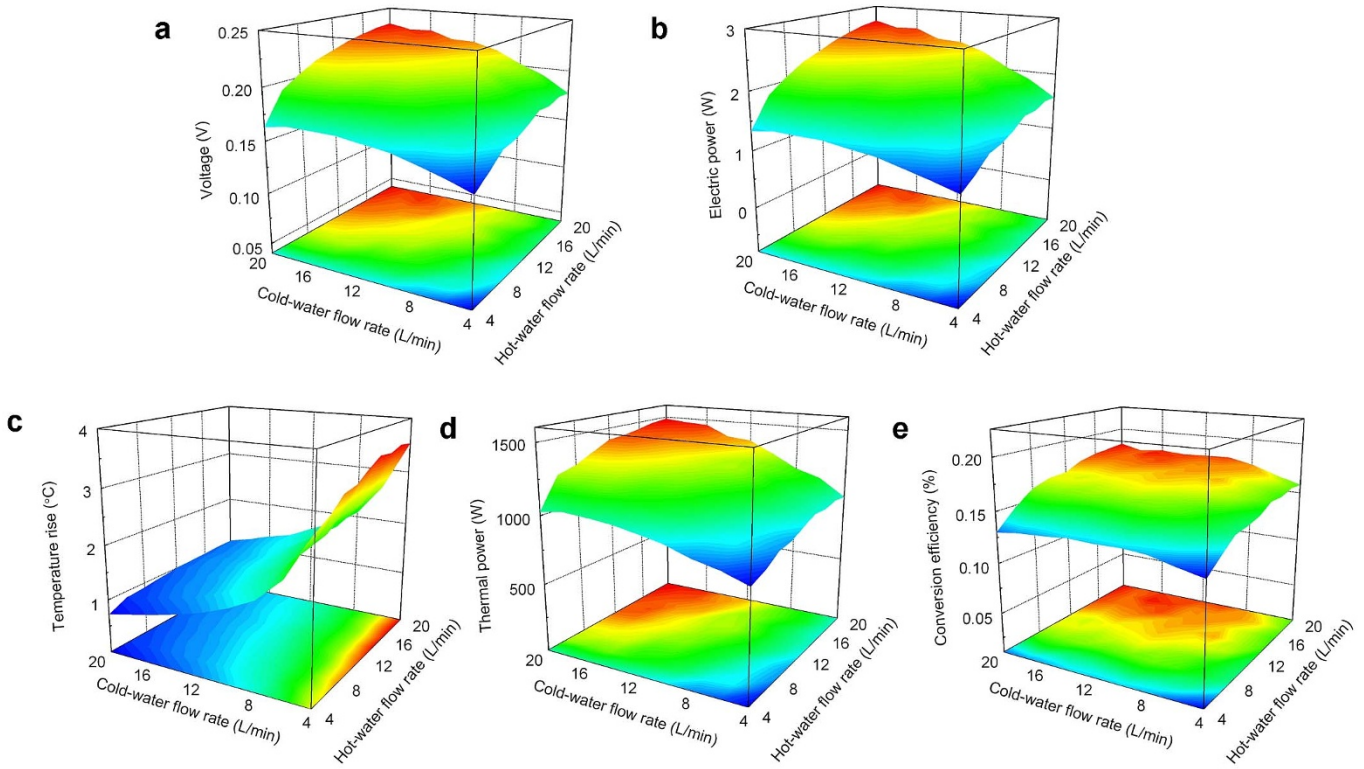

Figure 3 | Heat exchange properties and electric power generation properties of the BST/Ni multilayer tube. (a) V_{op}, (b) P_e, (c) T_{diff}, (d) Q, and (e) η measured as a function of F_{cw} and F_{hw}.

tubes were connected electrically in series and thermally in parallel. R_e of each BST/Ni tubes were 4.5–5 mΩ resulting in overall R_e of the TE generation unit of 19.5 mΩ. Hot-water at 95°C and cold-water at 10°C were introduced to the TE generation unit with total F_{hw} and F_{cw} of 32 L/min and 40 L/min, respectively. The hot and the cold-water are assumed to be equally distributed to each BST/Ni tube. Figure 4b shows the current-voltage plot and the power-voltage plot of the TE generation unit. The linear fit and the quadratic fit to each curve are also shown. Note that the data were taken by a pulsed source meter. We see that V_{op} is ~800 mV and P_e at load matching condition is as large as 8.1 W. Using a dc–dc voltage converter, we succeeded in operating various electronic products by this compact TE generation unit, such as LED light bulb, portable television, radio, and recharging of smart phones. The lighting of an LED light bulb is demonstrated in Fig. 4a. The volume power density of the TE generation unit was as large as 10 kW/m^3. The TE generation unit can further be scaled up easily in three dimensions, maintaining the compact and dense structure with the high-volume power density.

Discussion

We now discuss the validity of the present results by calculations based on an equivalent circuit model. In artificial tilted multilayer materials, the tensor components of the Seebeck coefficient S, electrical resistivity ρ, and thermal conductivity κ can be calculated by using the physical quantities of the constituent materials[13–17], in the present case, by using those of BST and Ni. The tensor components that govern the transverse TE properties of the tubular device are S_{xy}, ρ_{xx}, and κ_{yy}, where x and y corresponds to the direction along the radial direction and the axial direction of the tube, respectively[20]. The calculated TE quantities of the BST/Ni multilayer at room-temperature are summarized in Table 1 together with the measured TE quantities of BST and Ni. Note that the values of BST and Ni are those of individually pelletized samples fabricated by SPS under the same condition as that for fabricating the BST/Ni tube. The transverse ZT ($= S_{xy}{}^2T/\rho_{xx}\kappa_{yy}$) of the BST/Ni tube at room temperature can then estimated to be 0.144. However, since the equivalent circuit model considers stacking of an infinitely thin layers of BST and Ni, ZT of the actual layered structure, which has a finite layer thickness, is reduced from the abovementioned value as described in Ref. 20. In the present case, with the layer thickness and tube thickness of 1.3 mm and 2 mm, respectively, the reduction factor is estimated to be 0.4. Thus, ZT of the present BST/Ni tube is corrected to be 0.057. Using this calculated ZT, we can further calculate the theoretical η of the BST/Ni tube as[1],

$$\eta = \frac{\Delta T_{TE}}{T_{h,TE}} \frac{\sqrt{1+ZT}-1}{\sqrt{1+ZT}+T_{c,TE}/T_{h,TE}}, \quad (3)$$

where $T_{h,TE}$ and $T_{c,TE}$ is the temperature of the hotter side and the colder side of the tube, respectively, and ΔT_{TE} is $T_{h,TE} - T_{c,TE}$. The values of $T_{h,TE}$ and $T_{c,TE}$ were chosen here as 78°C and 26°C, respectively. This was determined by ΔT_{TE} ($= QR_t$) calculated by the Q measured at F_{hw} and F_{cw} of 20 L/min and the bulk-R_t deduced from the equivalent circuit model. The theoretical η is then calculated to be 0.216%. This value fairly agrees with that of the measured value of 0.189% at F_{hw} and F_{cw} of 20 L/min. The good agreement supports that the present tubular TE device operates on the basis of the transverse TE effect.

As suggested from the theory, η of the present BST/Ni tube is indeed relatively low. Nevertheless, the power density per heat transfer area achieved here (870 W/m^2) from the low-grade heat source below 100°C is comparable to that of the state-of-the-art π-shaped TE devices, which exhibit η of 4–5% at the same temperature range. This is due to the fact that the input-Q of the BST/Ni tube is about an order larger than that of the π-shaped TE devices. In the BST/Ni tube, the tubular structure enables direct heat transfer from the thermalized fluid to the TE material, and also, the high-κ of the Ni layer essentially reduces bulk-R_t of the BST/Ni tube. On the other hand, the π-shaped devices, besides their intrinsically high-R_t, have many interfacial thermal losses within their structure, and they also require indirect thermal transfer from the heat source via an external heat sink. The different heat exchange properties of the two devices results in similar P_e despite the large difference in η. Yet, we assume that the low-η of the present BST/Ni tube is not much of a problem for practical use considering that the amount of heat created in many industrial facilities is enormous, and that it is "waste heat" after all. Furthermore, in many of these facilities, TE generation is expected to be a residual product of cooling of a thermalized object. In this sense, the BST/Ni tube should be more advantageous for application to

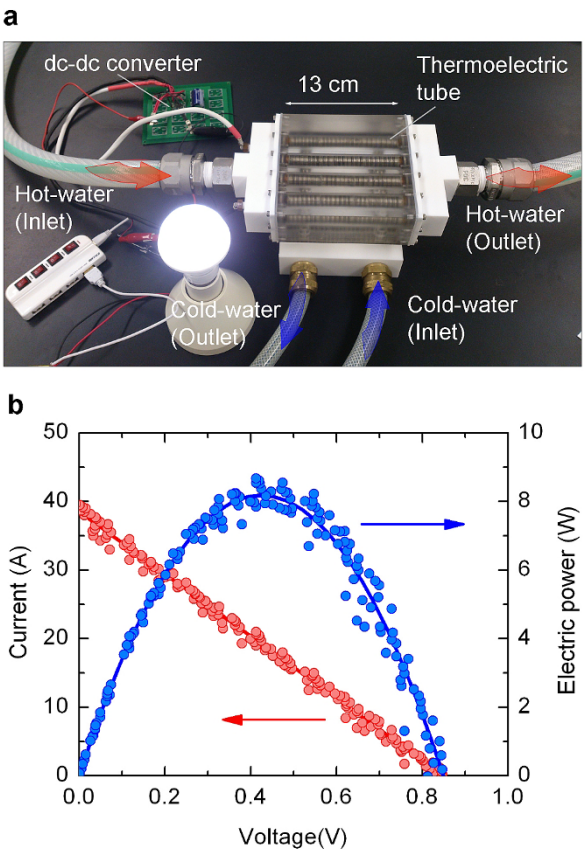

Figure 4 | Electric power generation from a compact TE generation unit made of multiple BST/Ni tubes. (a) Picture of a compact TE generation unit made of four BST/Ni tubes. (b) Current-voltage plot (closed squares) and power-voltage plot (closed circles) of the TE generation unit measured at T_{hw} of 95°C and T_{cw} of 10°C at F_{hw} of 32 L/min and F_{cw} of 40 L/min. The linear fit and the quadratic fit to each data are also shown by the solid lines. Demonstration of lighting of an LED light bulb is shown in (a) in its operation at the same condition.

Table 1 | Summary of the TE parameters (S, ρ, κ, and ZT at room temperature) of BST, Ni, and BST/Ni tilted multilayer. Note that the values of BST and Ni are those measured for individually pelletized samples at the same SPS condition used for fabricating the BST/Ni tube. The values of BST/Ni tilted multilayer are the tensor components calculated by the equivalent circuit model

	S (μV/K)	ρ (mΩcm)	K (W/mK)	ZT
$Bi_{0.5}Sb_{1.5}Te_3$	+210	1.1	1.4	0.859
Ni	−15	0.016	51	0.008
$Bi_{0.5}Sb_{1.5}Te_3$/Ni	+101	0.205	10.4	0.144

such scenes because it can serve as a heat exchanger aimed for cooling, and also a power generator making electricity at the same time. Nonetheless, we recognize that the π-shaped devices, due to their thermally insulative feature and relatively high-η, have advantages in power generation from limited or low-capacity heat sources, where cooling is less significant.

The tubular TE device made of tilted multilayer of BST/Ni thus achieves a perfect balance between high power generation and efficient heat exchange. The BST/Ni tube can be introduced simply by substituting the "tubes" in standard shell and tube heat exchangers already built-in the facilities. Therefore, additional expense necessary for its introduction is only its material cost, manufacturing cost, and some other cost for constructing the electrical system. This is in contrast to the TE heat exchangers examined on conventional π-shaped TE devices[21], which would require substitution of the entire heat exchange system. The multilayer TE tube can thus be cost-effective. Yet, we are aware that several issues still need to be taken care of before its practical use. One of the major concerns is the durability of the tube. Since the electrical current is exposed to water, electric corrosion can deteriorate the device performance. However, we have been testing the same BST/Ni tubes for several months, but performance deterioration has not been identified yet. Also, we have carried out water inspection of our water circulators, but none of the metal elements that compose the tube were detected. Further testing in a longer term will be necessary to clarify this issue. A thin surface coating layer may be preferred in the future for protection, also considering the toxicity of BST. Indeed, there are still things left to be improved, but the bifunctionality of the multilayer TE tube demonstrated here shall certainly provide a potential waste heat recovery solution in various industrial scenes.

Methods

Fabrication process of the BST/Ni tube. Powders of BST and Ni were pressed with tapered punches at room temperature into numbers of conical rings, each with an outer diameter of 14 mm and an inner diameter of 10 mm. Individual BST rings and Ni rings were alternately stacked one by one to form a hollow cylindrical shape (tubular shape) with a height of 5–6 cm. This structure was then processed by SPS at 500°C and 50 MPa to fabricate a dense BST/Ni tube with a height of 2.5–3.5 cm. The above processes were repeated four times to fabricate four short BST/Ni tubes. The four short BST/Ni tubes were then stacked and soldered with Sn-Bi paste to finally form a long BST/Ni tube with a total length of ~11 cm. The device was finalized by solder-pasting a 1.5 cm-long Cu joint tubes to both ends of the BST/Ni tube. The SPS-processed BST/Ni tube exhibited a firm and tightly sealed structure enabling leaktight fluid flow.

Experimental setup to measure the heat exchange properties and the power generation properties of the BST/Ni tube. The BST/Ni tube was placed inside an acrylic water jacket with a ϕ18 mm-flow channel. Hot-water supplied from a hot-water circulator was introduced inside the BST/Ni tube, while the outer side was cooled by introducing cold-water inside the acrylic water jacket using a water chiller. Teflon® water jackets were additionally attached to the acrylic water jacket to assist the water introduction. The inlet and the outlet water temperatures were measured by thermocouple sensors attached inside the Teflon® water jackets. Cu electrodes were screwed into the Teflon® hot-water jackets to make electric contact between the BST/Ni tube. A water flow meter was set in both the cold-water line and the hot-water line. The heat exchange properties and the power generation properties of the BST/Ni tube were evaluated by varying F_{cw} and F_{hw} from 4 to 20 L/min.

1. Snyder, G. J. & Toberer, E. S. Complex thermoelectric materials. *Nature Mater.* **7**, 105–114 (2008).
2. Bell, L. E. Cooling, heating, generating power, and recovering waste heat with thermoelectric systems. *Science* **321**, 1457–1461 (2008).
3. Dresselhaus, M. S. *et al.* New directions for low-dimensional thermoelectric materials. *Adv. Mater.* **19**, 1043–1053 (2007).
4. Majumdar, A. Thermoelectricity in semiconductor nanostructures. *Science* **303**, 777–778 (2004).
5. Nielsch, K., Bachmann, J., Kimling, J. & Böttner, H. Thermoelectric nanostructures: From physical model systems towards nanograined composites. *Adv. Energy Mater.* **1**, 713–731 (2011).
6. Poudel, B. *et al.* High-thermoelectric performance of nanostructured bismuth antimony telluride bulk alloys. *Science* **320**, 634–638 (2008).
7. Hochbaum, A. I. *et al.* Enhanced thermoelectric performance of rough silicon nanowires. *Nature* **451**, 163–167 (2008).
8. Boukai, A. I. *et al.* Silicon nanowires as efficient thermoelectric materials. *Nature* **451**, 168–171 (2008).
9. Lengfellner, H. *et al.* Giant voltages upon surface heating in normal $YBa_2Cu_3O_{7-\delta}$ films suggesting an atomic layer thermopile. *Appl. Phys. Lett.* **60**, 501–503 (1992).
10. Habermeier, H.-U., Li, X. H., Zhang, P. X. & Leibold, B. Anisotropy of thermoelectric properties in $La_{2/3}Ca_{1/3}MnO_3$ thin films studied by laser-induced transient voltages. *Solid State Commun.* **110**, 473–478 (1999).
11. Takahashi, K., Kanno, T., Sakai, A., Adachi, H. & Yamada, Y. Gigantic transverse voltage induced via off-diagonal thermoelectric effect in Ca_xCoO_2 thin films. *Appl. Phys. Lett.* **97**, 021906 (2010).
12. Goldsmid, H. J. Application of the transverse thermoelectric effects. *J. Electron. Mater.* **40**, 1254–1259 (2011).
13. Zahner, Th., Förg, R. & Lengfellner, H. Transverse thermoelectric response of a tilted metallic multilayer structure. *Appl. Phys. Lett.* **73**, 1364–1366 (1998).
14. Fischer, K., Stoiber, C., Kyarad, A. & Lengfellner, H. Anisotropic thermopower in tilted metallic multilayer structures. *Appl. Phys. A* **78**, 323–326 (2004).
15. Kyarad, A. & Lengfellner, H. Al-Si multilayers: A synthetic material with large thermoelectric anisotropy. *Appl. Phys. Lett.* **85**, 5613–5615 (2004).
16. Kyarad, A. & Lengfellner, H. Transverse Peltier effect in tilted Pb-Bi_2Te_3 multilayer structures. *Appl. Phys. Lett.* **89**, 192103 (2006).
17. Kanno, T., Yotsuhashi, S., Sakai, A., Takahashi, K. & Adachi, H. Enhancement of transverse thermoelectric power factor in tilted Bi/Cu multilayer. *Appl. Phys. Lett.* **94**, 061917 (2009).
18. Reitmaier, C., Walther, F. & Lengfellner, H. Power generation by the transverse Seebeck effect in Pb-Bi_2Te_3 multilayers. *Appl. Phys. A* **105**, 347–349 (2011).
19. Snyder, G. J. & Ursell, T. S. Thermoelectric Efficiency and Compatibility. *Phys. Rev. Lett.* **91**, 148301 (2003).
20. Kanno, T. *et al.* Tailoring effective thermoelectric tensors and high-density power generation in a tubular $Bi_{0.5}Sb_{1.5}Te_3$/Ni composite with cylindrical anisotropy. *Appl. Phys. Lett.* **101**, 011906 (2012).
21. Kristiansen, N. R., Snyder, G. J., Nielsen, H. K. & Rosendahl, L. Waste heat recovery from a marine waste incinerator using a thermoelectric generator. *J. Electron. Mater.* **41**, 1024–1029 (2012).

Acknowledgments

A part of this work belongs to "Research and Development of Thermoelectric Devices for Independent Systems Project" contracted with New Energy and Industrial Technology Development Organization (NEDO).

Author contributions

K.T. performed the measurements and drafted the manuscript which was further revised by all authors. A.S., H.T. and H.K. fabricated the BST/Ni tube. T.K. developed a calculation model based on equivalent circuit. T.K. and Y.Y. directed the work.

Additional information

Competing financial interests: The authors declare no competing financial interests.

How to cite this article: Takahashi, K. *et al.* Bifunctional thermoelectric tube made of tilted multilayer material as an alternative to standard heat exchangers. *Sci. Rep.* **3**, 1501; DOI:10.1038/srep01501 (2013).